Biointerface Research in Applied Chemistry
Open-Access Journal (ISSN: 2069-5837)

Article
Volume 13, Issue 1, 2023, 48
https://doi.org/10.33263/BRIAC131.048

Structural, Thermal and Physical Properties of the Calcium Borovanadate Glasses Belonging to the 40CaO-(60-x)B_2O_3-xV_2O_5 System

Ayoub Kaaouass [1], Abdelkader Ben Ali [1], Fouad Alloun [1], Abdelkader Zarrouk [2,*], Mohamed Saadi [1]

[1] Laboratoire de Chimie Appliquée Des Matériaux (LCAM), Faculty of Science, Mohammed V University in Rabat, P.O. Box. 1014 Agdal-Rabat, Morocco;
[2] Laboratory of Materials, Nanotechnology and Environment, Faculty of Sciences, Mohammed V University in Rabat, P.O. Box. 1014 Agdal-Rabat, Morocco;
* Correspondence: azarrouk@gmail.com (A.Z.);

Scopus Author ID 36125763200
Received: 3.11.2021; Accepted: 15.12.2021; Published: 30.01.2022

Abstract: The calcium borovanadate glasses within the system 40CaO-(60-x)B_2O_3 -xV_2O_5 with x= 0, 5, 10, 15, 20, 30, 40 mol% was studied. The glass samples were elaborated via melting, followed by quenching. Its structural, thermal, and physical properties were explored. Powder X-ray diffraction was used to demonstrate that the developed glasses were amorphous. The influence of vanadium, a 3d transition element, on physical characteristics such as density and molar volume was investigated. The variation of density and molar volume has been discussed in terms of the structural changes in the vitreous matrix with adding the V_2O_5. Infrared (FTIR) and Raman spectroscopies were done to check the group constitution of the glass. This analysis shows that the vitreous materials are mainly established from BO_4 and BO_3 units with four and five coordinated vanadium in all glasses containing V_2O_5, confirmed with the density results. Moreover, it is found from the infrared spectra the existence of diborovanadate $[B_2V_2O_9]^{2-}$ in glass samples with composition x =15, 20, 30, 40.

Keywords: borovanadate; glass; vanadium oxide; transition temperature; spectroscopic studies.

1. Introduction

Borates are well-known as one of the greatest materials for creating glass. Furthermore, because boron atoms may be accommodated in both trigonal and tetrahedral settings, anionic sites can be created to accommodate various modified metal cations [1,2].

XRD, FTIR, Raman, and UV-visible spectroscopies have all been used to investigate the structural, optical, and physical properties of borovanadate glasses [1,3–6].

Furthermore, the addition of oxide-based transition elements such as V_2O_5, MoO_3, TiO_2, Fe_2O_3, WO_3, ZnO, etc., to oxide glasses are known to exhibit semiconducting behavior. Transition-element glasses have been extensively studied due to their numerous applications, including optical and electrical memory switching, active cathode material for solid-state device construction, and optical fiber assembly [4,7–10].

Vanadium is a significant semiconductor among transition metals because of the electron hopping between V^{5+} and V^{4+} ions [7]. Vanadium ions are suggested to exist in the glass materials in three possible oxidation states: tri-, tetra-, and pentavalent states [7,9,11,12].

Glass is not formed by transition metal oxides (Bi_2O_3, TeO_2, MoO_3, V_2O_5, WO_3, etc.). They can easily create a glass when combined with a second glass-forming oxide. A stronger glass network could be achieved by combining different glass-forming techniques. When a modifier oxide like B_2O_3 or V_2O_5 is added to glasses with two formers, the environment and connection of the borate and vanadate species might vary dramatically [5,13].

Considerable work has been done on the borate glasses holding V_2O_5 [1,3–7,11]; nonetheless, the glasses containing CaO, B_2O_3, and V_2O_5 together are found very few. Divalent cations like Ca^{2+}, Zn^{2+}, Pb^{2+}, Ba^{2+}, etc., play a significant key in both formation and modification of local structure [5]. CaO was chosen to be used in glass materials in some previous studies for their bioglass properties. Bioactive glass is composed of many elements of the human body, which Ca is one of them; for that reason, it has an interesting role in bioglasses [14–16].

Recent studies on borovanadate glasses show that in binary vanadium borate glasses [11], the vanadium adopts tetrahedral or penta-hededral environments while boron is mainly in diborate pyroborate groups using spectroscopy technics. In their unique vibrational modes, the bands of all generated glasses exhibit both triangular BO_3 groups and tetrahedral BO_4 groups; however, transition metal ions have a limited impact due to the low doping concentration (0, 2 percent). In the infrared spectra of lead borovanadate glass [5], the characteristic band corresponding to B–O–B, V–O–V, B–O–V, and B–O–V vibrations can be seen, indicating the creation of advanced structural groups such as diborovanadate $[B2V2O9]^{2-}$ and four coordinated boron atoms.

X-Ray Diffraction (XRD), Density Measurement, Differential Scanning Calorimetry (DSC), Scanning Electron Microscopy (SEM), Fourier Transform Infrared (FT-IR), and Raman Spectroscopy have been used in this work to study the structural, thermal, and physical properties as a function of V_2O_5 concentration $40CaO–(60-x)B_2O_3 -xV_2O_5$ ($0 \leq x \leq 40$) glasses.

2. Materials and Methods

2.1. Sample preparation.

$40CaO–(60-x)B_2O_3 -xV_2O_5$ (with x = 0, 5, 10, 15, 20, 30, 40 mol %) are prepared by melt quench method. Vanadium oxide (V_2O_5), boric acid (H_3BO_3), and calcium carbonate ($CaCO_3$) were used as raw materials. These reagent masses are accurately weighed, then mixed, and thoroughly ground to homogenize the mixture before being gradually heated in a crucible at 400 °C. Depending on the composition, the mixtures were melted at 900–950 °C for about 60 min before being quenched into a preheated steel mold. The composition of the seven elaborated glasses in this study is summarized in Table 1.

Table 1. Glass composition (molar %) with sample labels.

Glass	CaO	B_2O_3	V_2O_5
CBV0	40	60	0
CBV1	40	55	5
CBV2	40	50	10
CBV3	40	45	15
CBV4	40	40	20
CBV5	40	30	30
CBV6	40	20	40

2.2. X-ray diffraction analysis.

The amorphous/crystalline condition of the produced samples was determined by powder X-ray diffraction (XRD) using a LabxXRD-6100 Shimadzu diffractometer at a scanning rate of 2 degrees/min and 2 varied between 10–70° with a CuKα radiation source.

2.3. Physical parameters measurement.

The Archimedes principle was used to compute the density of glasses using Diethyl phthalate ($C_{12}H_{14}O_4$) as an immersion liquid, in which sample weights are assessed in both air and Diethyl phthalate. The density of the glass ($\boldsymbol{\rho}$) is determined by using the following formula:

$$\rho = \frac{\boldsymbol{W_A}}{\boldsymbol{W_A - W_B}} \times \rho_{liquid} \qquad \text{Eq (1)}$$

W_A is the weight of the sample in air, W_B is the immersed weight of the sample in Diethyl phthalate, and ρ_{liquid} is the density of the Diethyl phthalate (1.120 g/cm^3).

The molar volume (V_M) of each glass was then calculated using the equation and the density of the glass.

$$V_M = \frac{M}{\rho_{glass}} \qquad \text{Eq (2)}$$

where M denotes the molecular weight of glass and ρ_{glass} glass denotes its density.

2.4. Thermal behavior of prepared glasses.

The glass transition temperature (Tg) was determined in an argon environment using a Setaram121 equipment and differential scanning calorimetry at a heating rate of 10 °C/min (DSC).

2.5. Structural investigation.

The local environment of the boron and vanadium atoms in elaborated glasses has been studied using infrared and Raman spectroscopies. The infrared transmission spectra of the glasses were measured at room temperature in the wavenumber range 4000–400 cm^{-1} with a Bruker Platinium-ATR apparatus.

The samples Raman spectra were obtained at room temperature using a DXR2 Smart Raman Spectrometer and a laser source (633nm) as the excitation light; the laser power at the sample surface was 6.1 mW. The spectra were recorded between 100 and 3500 cm^{-1}.

2.6. Microstructural characterization.

The microstructure of glasses has been explored via A QUANTA scanning electron microscope (SEM). The solid pieces were studied on carbon substrates.

3. Results and Discussion

3.1. X-ray diffraction.

The X-ray diffraction pattern of the studied glasses inside the $40CaO–(60\text{-}x)B_2O_3$ - xV_2O_5 ($0 \leq x \leq 40$) system is given in Figure 1. This analysis reveals that all the prepared samples are completely amorphous due to the absence of peaks where the spectra reveal the

only hump around 2θ ~ 28–29. The absence of sharp and strongly diffracted beams in the X-ray diffraction diagrams clearly indicates the amorphous nature [7,17].

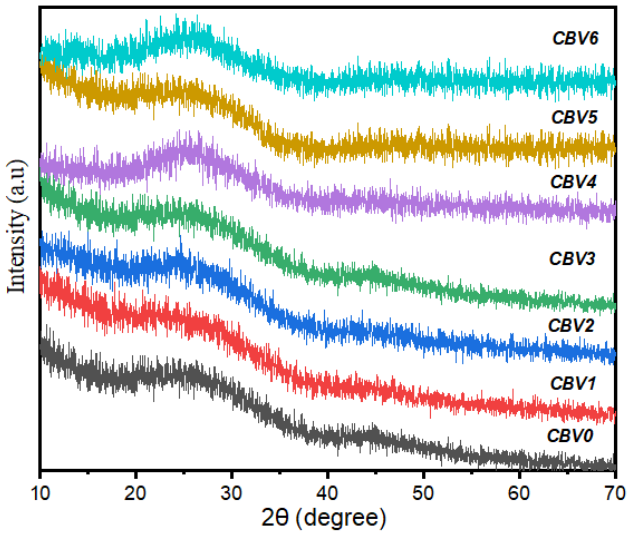

Figure 1. XRD of the obtained glasses in the 40CaO–(60-x)B_2O_3 -xV_2O_5 ($0 \leq x \leq 40$) system.

3.2. Glass transition temperature, density, & molar volume.

Density of the 40CaO-xV_2O_5–(60-x)B_2O_3 ($0 \leq x \leq 40$) glasses (Table 2 and Figure 2) , depends strongly on the content of highest mass substance. The molecular weight of V_2O_5 (181.88 g/mol) is higher than that of B_2O_3 (69.62 g/mol); thus, the density of V_2O_5 (3.36 g/cm^3) is also higher than that of B_2O_3 (1.82 g/cm^3) [11]. Therefore, the density of the prepared glasses increases from 2.60 to 2.91 g/cm^3 with increasing of the V_2O_5 content from 0 to 40 mol%, which are in good agreement with the previously reported results [11,18].

Additional oxygen is available from V_2O_5, which causes the coordination of BO_3 to BO_4 to shift [19]. Can explain why the presence of V_2O_5 increases the density of glass. Because the tetrahedral BO_4 units are more tightly coupled than the triangular BO_3 units, a compact structure with a higher density is expected [7,20,21]. Furthermore, increasing density with the addition of V_2O_5 could be attributed to the formation of VO_4 and VO_5 groups. Thus, the incorporation of V_2O_5 has adjusted the borate glass structure by creating more BO_4, VO_4, and VO_5 groups.

However, as the V_2O_5 content climbed from 0 to 40 mol percent, the developed glasses' molar volume increased from 24.66 to 37.44 cm^3/mol (Table 2 and Figure 2). Generally, density and molar volume are usually expected to present opposite behavior, but this is not the case in these investigated glasses. Nonetheless, several other investigations [11,22–26] have demonstrated this strange relationship between density and molar volume.

The variation of density and molar volume with V_2O_5 mol% was presented in Figure 2.

Table 2. Density (ρ), molar volume (V_M), and glass transition temperature (Tg) for all elaborated glasses.

Glass	ρ (gm/cm^3)	V_M (cm^3/mol)	Tg (°C)
CBV0	2.603	24.664	650.95
CBV1	2.637	26.481	610.28
CBV2	2.669	28.264	570.31
CBV3	2.716	29.841	530.20
CBV4	2.749	31.524	480.81
CBV5	2.853	34.313	430.95
CBV6	2.914	37.438	381.12

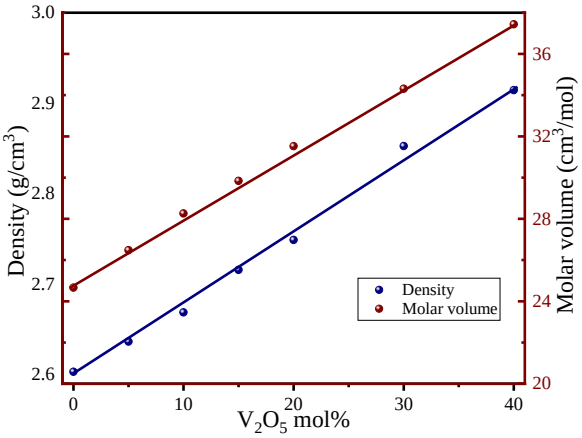

Figure 2. Variation of density and molar volume with V_2O_5 mol%.

The glass structural adjustment (Tg) affects the glass transition temperature, and the construction of thermally stable glasses is dense [22]. Figure 3 shows the DSC curves of several glass samples 40CaO–(60-x)B_2O_3 xV_2O_5 with x=5, 10, 15, 30.

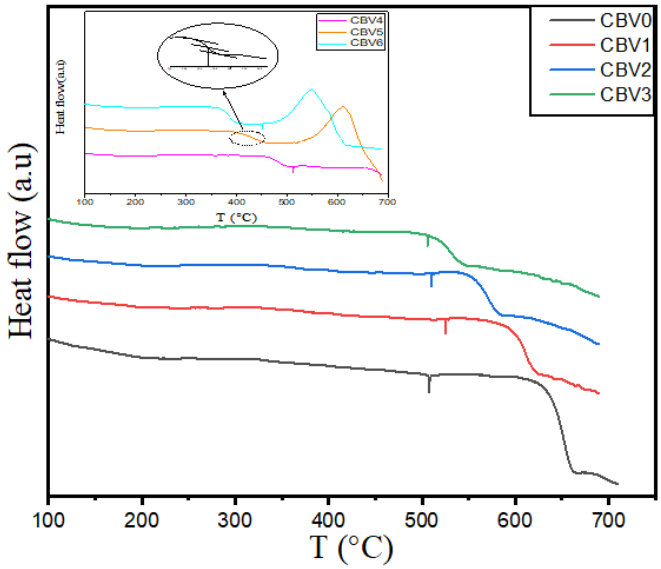

Figure 3. Differential scanning calorimetric curves of the glass samples.

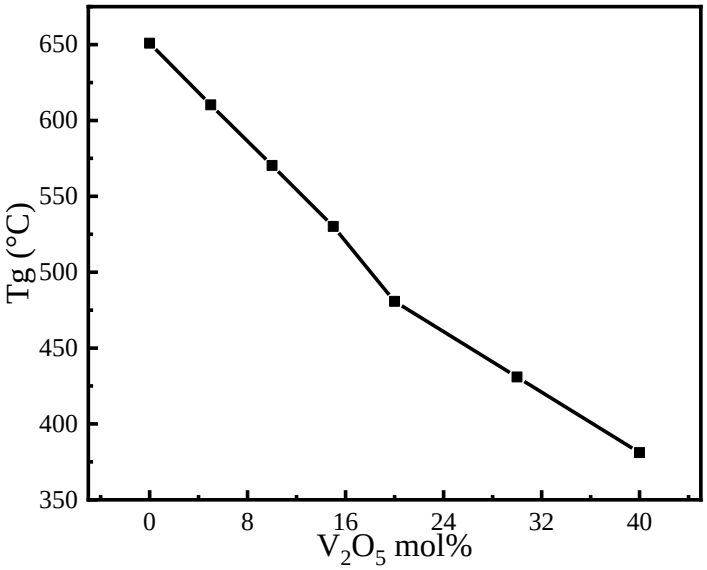

Figure 4. Variation of glass transition temperature with V_2O_5 content.

The evolution of Tg in the function of V_2O_5 concentration is illustrated in Figure 4; the values of the glass transition temperatures are listed in Table 2. As can be depicted from this variation, the Tg temperature decreases from 650.95 to 381.12 °C with increase in the concentration of vanadium oxide V_2O_5. The increase in V_2O_5 content causes a decrease in Tg and an increase in molar volume. As a result, the Tg values vary, indicating that an increase in V_2O_5 content weakens the network structure by causing more voids in the glass matrix [22]. According to Roy, the molar volume impacts Tg more than the binding strength [22]. Reddy *et al*. [5] observed the same behavior when they added PbO to borovanadate glasses. The Tg increases straightly with the percentage of PbO and decreases with increasing V_2O_5 demonstrating that the conversion of three coordinated boron atoms into four coordinated boron atoms affects the Tg [5].

3.3. FTIR spectra analysis.

Figure 5 shows the infrared transmittance spectra for different compositions of calcium borovanadate glasses recorded in the 4000-400 cm^{-1} region.

According to the literature, the vibrational modes of the borate network are located in three regions of the infrared spectrum [6,7,27–29]. Due to the bending of B-O-B links in borate networks, the first is positioned at approximately 700 cm^{-1} [5,28,29]. The second area, roughly 800-1200 cm^{-1}, corresponds to the tetrahedral BO4 units B-O bond stretching [1,4,11,30,31]. The stretching relaxation of the trigonal BO_3 units B-O band [27,28,32] and stretching of trigonal boron found in $[B_2V_2O_9]^{2-}$ [5,12,13,33] is responsible for the third area, which lies between 1200 and 1600 cm^{-1}.

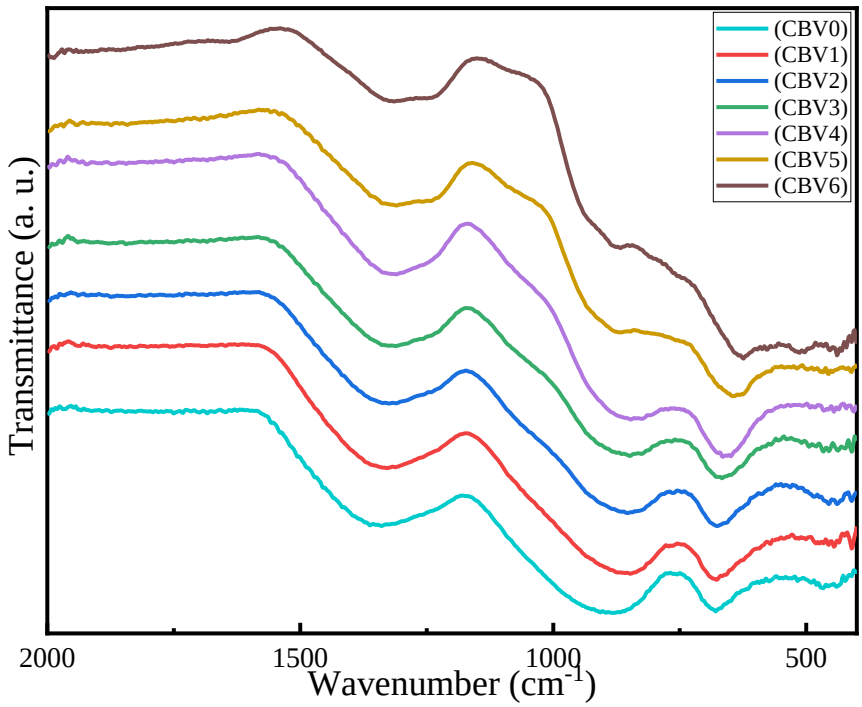

Figure 5. Infrared spectrum for all the prepared glasses.

The observed IR bands for the $40CaO–(60-x)B_2O_3$ $-xV_2O_5$ ($0 \leq x \leq 40$) glass are presented in Table 3.

No peak has been observed in the 4000–1500cm^{-1} region. All elaborated glasses exhibit bands in the 1200-1600 region, the peak with maxima situated at 1350 cm^{-1} is assigned to the

B−O vibration in [BO_3] [32,34–38], the second band in the 1200-1600 region with the maxima at 1230 cm^{-1} begins to appear when the molar content of V_2O_5 exceeds 15%, This could be explained by the trigonal boron bending in $[B_2V_2O_9]^{2-}$ [5,13,33].. The presence of B-O vibrations (band situated at 1230) in the glasses containing more than 15 mol% of V_2O_5, indicate the occurrence of the diborovanadate groups $[B_2V_2O_9]^{2-}$, the formation of diborovanadate groups is elucidated by supposing that in glasses containing more than 15 mol% of V_2O_5, a continuous random network is formed of either two BO_4 units and two VO_4 units (type 1) or two BO_3 units and two VO_5 units (type 2), the same building was proposed by Reddy and his collaborators for diborovanadate $[B_2V_2O_9]^{2-}$ [5,13,33].

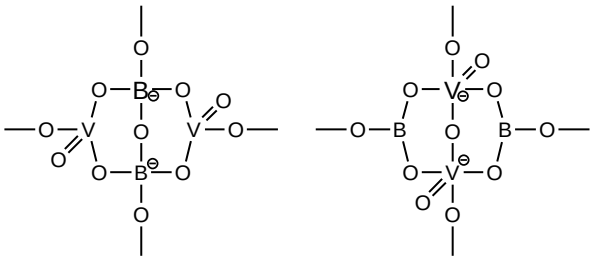

Type 1 **Type 2**

Figure 6. Diborovanadates groupements $[B_2V_2O_9]^{2-}$ (according to reddy *et al*. [5]).

The band situated from 848 to 890 cm^{-1} can be assigned to the vibration B-O in BO_4 unit [38–42]. Its corresponding intensity decreases with increasing of V_2O_5 percentage. When the concentration of V_2O_5 increases from 15% to 40%, the observed peak shifts from 848 to 882 cm^{-1}, which is probably related to the V-O stretching of the VO_4 group [7]. According to Arya *et al*.[3], the movement of bands may be caused by the structural changes related to the variation of bond angles.

A very weak peak at around 680 cm^{-1} was presented in all the elaborated glasses accorded to B-O–B linkage in the borate networks [40,43,44]. This peak shifts to 622 cm^{-1} with increasing vanadium oxide concentration in the glass. This behavior may be related to grouping the vibration bands of the B-O-V and B-O-B bonds present respectively in vanadate and borate glasses [5,13].

Table 3. Observed IR and Raman bands in $40CaO–(60-x)B_2O_3$ $-xV_2O_5$ ($0 \leq x \leq 40$) glasses.

Glass	Peaks positions (cm-1)					
CBV0	IR	680	890	-	1350	
	RAMAN	555	775	-	-	1289
CBV1	IR	680	861	-	1334	-
	RAMAN	580	775	930	1104	-
CBV2	IR	675	855	-	1328	-
	RAMAN	565	775	935	1104	-
CBV3	IR	667	848	1217	1319	-
	RAMAN	565	775	942	1104	-
CBV4	IR	661	861	1223	1311	-
	RAMAN	565	775	947	1104	-
CBV5	IR	639	873	1225	1311	-
	RAMAN	565	775	947	1104	-
CBV6	IR	626	882	1230	1311	-
	RAMAN	565	786	947	1104	-

3.4. RAMAN spectroscopy analysis.

Figure 7 and Table 4 presents the Raman spectrum of all elaborated glass samples in the region of 100-2000 cm-1 and the Raman shift of the observed bands, respectively. From

the sample without vanadium CBV0, the major Raman bands are observed at 555 cm^{-1}, 786 $cm^{-1,}$ and 1280 cm^{-1}. When adding the V_2O_5, two-band at 930 cm^{-1} and 1104 cm^{-1} appear; the band at 930cm^{-1} shifts up to 947 cm^{-1} and becomes even stronger as V_2O_5 content rises. A band at 1280 cm^{-1} disappeared when V_2O_5 was added.

From Raman spectra of borate calcium glass CBV0, a strong peak observed at 1286 cm^{-1} result from the contribution of B–O stretching vibrations in trigonal arrangements such pyroborate composed by boroxol [45–48].

The absence of a peak in the range of 930-947 cm^{-1} for the CBV0 glass is ordinary in that there is no V = O bond, whereas when we add the V_2O_5 this peak begins to appear, which is attributed to the V=O vibrations of tetrahedral VO_4 or VO_5 units [49,50].

It is known from many studies [45,47,48] that the bands at around 1075-1150 cm^{-1} consist of diborate groups. Consequently, in this work, the observed band at 1104 cm^{-1} was attributed to the diborate groups [45–47,51].

In addition, all the synthesized glass samples exhibit bands around 555 and 775 cm^{-1}, these peaks attest to the presence of the B-O-B stretching in the BO_4 units (pentaborate) [42,46,48,51]. The band present at 775 cm^{-1} is characteristic of six-member rings with one or two BO_3 triangles replaced by BO_4 tetrahedra [47,49,51,52].

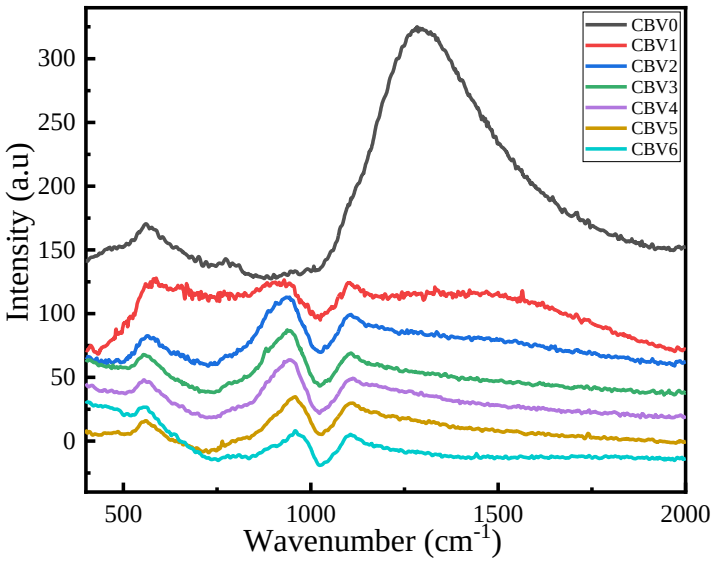

Figure 7. Raman spectrum for all the glass samples.

3.5. Scanning electron microscopy (SEM).

The morphology of the prepared glass samples is performed by scanning electron microscopy (SEM). Figure 8 illustrates the SEM images of the 40CaO–(60-x)B_2O_3 -xV_2O_5 samples with x=0 and 10%. As shown, the samples under investigation CBV0 and CBV2 indicate good homogeneity and smooth surface in sheets.

4. Conclusions

The physical, thermal and structural properties have been investigated for the 40CaO-xV_2O_5–(60-x)B_2O_3 ($0 \leq x \leq 40$) glasses. The X-ray diffraction method confirmed the amorphous state of the elaborated glasses.

The density values and molar volume of glasses rise as V_2O_5 content increases, implying the existence of more oxygen from V_2O_5 that moves the coordination of BO_3 to BO_4;

adding the V_2O_5 more groups of BO_4, VO_4, and VO_5 are created. It is observed from DSC studies that Tg decreases with increasing V_2O_5, which can be attributed to a transformation of BO_3 to BO_4.

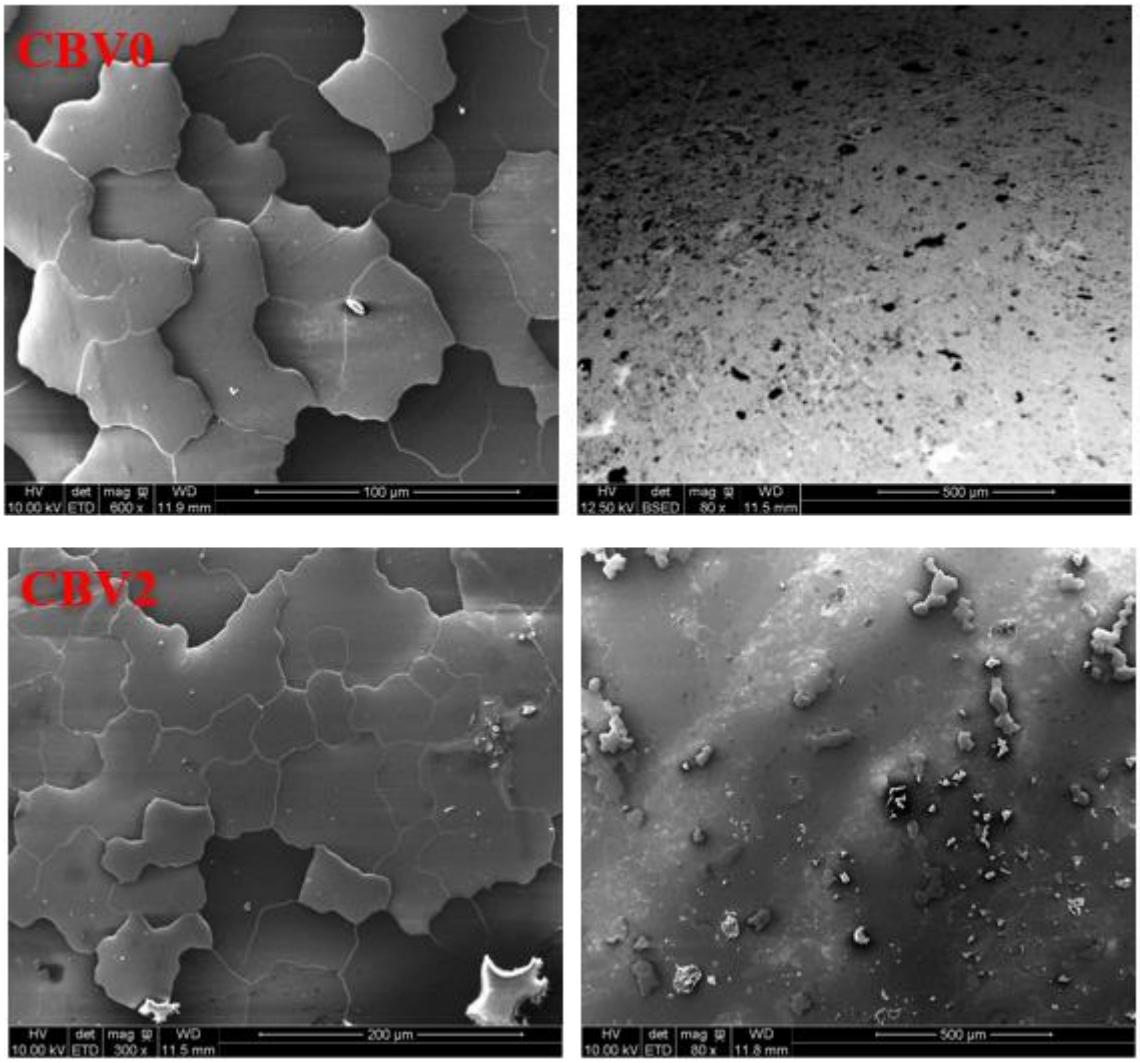

Figure 8. SEM Micrographs of CBV0 and CBV2 glass samples.

From the FT-IR results, it is clear for calcium and borate binary glass that we have the existence of the BO_3 and BO_4 groups. When V_2O_5 with different percentages is added, BO_3 group starts converting into BO_4 groups, and VO_4 groups start to appear, thereby the presence of diborovanadate units. This shows that V_2O_5 is present in the glass structure as a network former and a modifier. Raman spectroscopy confirms the conversion of BO_3 to BO_4, and the presence of VO_4 or VO_5 in glasses containing V_2O_5, diborate, pyroborate, and pyroborate are observed from Raman spectra.

Funding

This research received no external funding.

Acknowledgments

We thank all colleagues.

Conflicts of Interest

The authors declare no conflict of interest.

References

1. Abdelghany, A.M.; Hammad, A.H. Impact of Vanadium Ions in Barium Borate Glass. *Spectrochimica Acta Part A: Molecular and Biomolecular Spectroscopy* **2015**, *137*, 39–44, https://doi.org/10.1016/j.saa.2014.08.012.
2. Barebita, H.; Ferraa, S.; Moutataouia, M.; Baach, B.; Elbadaoui, A.; Nimour, A.; Guedira, T. Structural Investigation of Bi2O3-P2O5-B2O3-V2O5 Quaternary Glass System by Raman, FTIR and Thermal Analysis. *Chemical Physics Letters* **2020**, *760*, https://doi.org/10.1016/j.cplett.2020.138031.
3. Arya, S.K.; Kaur, G.; Singh, K. Effect of Vanadium on the Optical and Physical Properties of Lithium Borate Glasses. *Journal of Non-Crystalline Solids* **2016**, *432*, 393–398, https://doi.org/10.1016/j.jnoncrysol.2015.10.037.
4. ElBatal, H.A.; Abdelghany, A.M.; Ghoneim, N.A.; ElBatal, F.H. Effect of 3d-Transition Metal Doping on the Shielding Behavior of Barium Borate Glasses: A Spectroscopic Study. *Spectrochimica Acta Part A: Molecular and Biomolecular Spectroscopy* **2014**, *133*, 534–541, https://doi.org/10.1016/j.saa.2014.06.044.
5. Reddy, C.N.; Gowda, V.C.V.; Chakradhar, R.P.S. Elastic Properties and Structural Studies on Lead–Boro–Vanadate Glasses. *Journal of Non-Crystalline Solids* **2008**, *354*, 32–40, https://doi.org/10.1016/j.jnoncrysol.2007.07.011.
6. Sindhu, S.; Sanghi, S.; Agarwal, A.; Seth, V.P.; Kishore, N. Structural, Optical, Physical and Electrical Properties of V2O5·SrO·B2O3 Glasses. *Spectrochimica Acta Part A: Molecular and Biomolecular Spectroscopy* **2006**, *64*, 196–204, https://doi.org/10.1016/j.saa.2005.06.039.
7. Singh, G.P.; Kaur, P.; Kaur, S.; Singh, D.P. Role Of V2o5 In Structural Properties Of V2O5-MnO2-PbO-B2O3 Glasses. *Materials Physics and Mechanics* **2011**, *12*, 58–63.
8. Chand, P.; Kumar, L.; Khasa, S. Density and FTIR Study of Fe2O3 – V2O5 – Na2O – B2O3 Dilute Magnetic Glasses .AIP Conference Proceedings 2265, Jodhpur, India, 18–22 December 2019; Veerendra, K.; Sharma, C.L.P.; Yusuf , S.M. **2020**; https://doi.org/10.1063/5.0016946.
9. Saetova, N.S.; Raskovalov, A.A.; Antonov, B.D.; Denisova, T.A.; Zhuravlev, N.A. Structural Features of Li2O–V2O5–B2O3 Glasses: Experiment and Molecular Dynamics Simulation. *Journal of Non-Crystalline Solids* **2020**, *545*, https://doi.org/10.1016/j.jnoncrysol.2020.120253.
10. Kilic, G.; Ilik, E.; Mahmoud, K.A.; El-Agawany, F. I.; Alomairy, S.; Rammah, Y.S. The Role of B2O3 on the Structural, Thermal, and Radiation Protection Efficacy of Vanadium Phosphate Glasses. *Appl. Phys. A* **2021**, *127*, https://doi.org/10.1007/s00339-021-04409-9.
11. Laorodphan, N.; Pooddee, P.; Kidkhunthod, P.; Kunthadee, P.; Tapala, W.; Puntharod, R. Boron and Pentavalent Vanadium Local Environments in Binary Vanadium Borate Glasses. *Journal of Non-Crystalline Solids* **2016**, *453*, 118–124. https://doi.org/10.1016/j.jnoncrysol.2016.10.005.
12. Sivasankara Reddy, N. Role of Zinc Sulfate on Thermal and Mechanical Properties of Borovanadate Glasses. *Materials Today: Proceedings* **2021**, https://doi.org/10.1016/j.matpr.2021.05.292.
13. Reddy, C.N.; Damle, R.; Anavekar, R.V. Spectroscopic and Structural Studies on Calcium Borate Glasses Containing V2_O_5. *Physics and Chemistry of Glasses* **2006**, *47*, 34–40.
14. Jones, J.R.; Brauer, D. S.; Hupa, L.; Greenspan, D.C. Bioglass and Bioactive Glasses and Their Impact on Healthcare. *Int J Appl Glass Sci* **2016**, *7*, 423–434, https://doi.org/10.1111/ijag.12252.
15. Er-Rouissi, Y.; Aqdim, S.; El Bouari, A.; Hmimid, F.; Aqdim, S. Chemical Durability, Structure Properties and Bioactivity of Glasses. *AMPC* **2020**, *7*, 353–363, https://doi.org/10.4236/ampc.2020.1012024.
16. Tekin, H.O.; Al-Buriahi, M.S.; Issa, S.A.M.; Zakaly, H.M.H.; Issa, B.; Kebaili, I.; Badawi, A.; Karim, M.K.A.; Matori, K.A.; Zaid, M.H.M. Effect of Ag2O Substituted in Bioactive Glasses: A Synergistic Relationship between Antibacterial Zone and Radiation Attenuation Properties. *Journal of Materials Research and Technology* **2021**, *13*, 2194–2201, https://doi.org/10.1016/j.jmrt.2021.06.025.
17. Nidzam, N.N.S.; Kamari, H.M.; Sukari, M.S.M.; Alauddin, F.A.M.; Laoding, H.; Azlan, M.N.; Hann, S.W.; Al-Hada, N.M.; Boukhris, I. Comparison Study of Elastic, Physical and Structural Properties for Strontium Oxide and Manganese Oxide in Borotellurite Glasses for High Strength Glass Application. *Journal of Inorganic and Organometallic Polymers and Materials* **2021**, https://doi.org/10.21203/rs.3.rs-772802/v1.
18. Sharma, B.K.; Dube, D.C.; Mansingh, A. Preparation And Characterisation Of V2o5-B203 Glasses. *Journal of Non-Crystalline Solids* **1984**, *65*, 39–51, https://doi.org/10.1016/0022-3093(84)90353-3.
19. Mahmoud, K.H.; Alsubaie, A.S.; Wahab, E.A.A.; Abdel-Rahim, F.M.; Shaaban, K.S. Research on the Effects of Yttrium on Bismuth Titanate Borosilicate Glass System. *Silicon* **2021**, https://doi.org/10.1007/s12633-021-01125-0.
20. Singh, D.; Singh, K.; Bajwa, B. S.; Mudahar, G. S.; Singh, D. P.; Manupriya; Arora, M.; Dangwal, V. K. Optical and Structural Properties of Li2O–Al2O3–B2O3 Glasses before and after γ-Irradiation Effects. *Journal of Applied Physics* **2008**, *104*, https://doi.org/10.1063/1.3003070.

21. Singh, D.; Singh, K.; Singh, G.; Manupriya; Mohan, S.; Arora, M.; Sharma, G. Optical and Structural Properties of ZnO–PbO–B $_2$ O $_3$ and ZnO–PbO–B $_2$ O $_3$ –SiO $_2$ Glasses. *J. Phys.: Condens. Matter* **2008**, *20*, https://doi.org/10.1088/0953-8984/20/7/075228.
22. Gaafar, M.S.; Afifi, H.A.; Mekawy, M.M. Structural Studies of Some Phospho-Borate Glasses Using Ultrasonic Pulse–Echo Technique, DSC and IR Spectroscopy. *Physica B: Condensed Matter* **2009**, *404*, 1668–1673, https://doi.org/10.1016/j.physb.2009.01.045.
23. Saddeek, Y.B.; Latif, Lamia. A.E. Effect of TeO2 on the Elastic Moduli of Sodium Borate Glasses. *Physica B: Condensed Matter* **2004**, *348*, 475–484, https://doi.org/10.1016/j.physb.2004.02.001.
24. Kurtulus, R.; Sayyed, M. I.; Kavas, T.; Mahmoud, K.A.; Tashlykov, O.L.; Khandaker, M.U.; Bradley, D.A.A Lanthanum-Barium-Borovanadate Glass Containing Bi2O3 for Radiation Shielding Applications. *Radiation Physics and Chemistry* **2021**, *186*, https://doi.org/10.1016/j.radphyschem.2021.109557.
25. Alothman, M.A.; Kurtulus, R.; Olarinoye, I.O.; Kavas, T.; Mutuwong, C.; Al-Buriahi, M.S. Optical, Elastic, and Radiation Shielding Properties of Bi2O3-PbO-B2O3 Glass System: A Role of SnO2 Addition. *Optik* **2021**, *248*, https://doi.org/10.1016/j.ijleo.2021.168047.
26. Goel, P.; Honnavar, G.V. Short-Range Structural Insight into Lithium-Substituted Barium Vanadate Glasses Using Raman and EPR Spectroscopy as Probes. *ACS Omega* **2021**, *6*, 22454–22461, https://doi.org/10.1021/acsomega.1c03544.
27. Abou Hussein, E. Gamma Rays Interactions on Optical, FTIR and ESR Spectra of Alkaline Earth Binary Borate Glasses. *Arab Journal of Nuclear Sciences and Applications* **2020**, *53*, 1–18, https://doi.org/10.21608/ajnsa.2020.17460.1278.
28. karumuri, V. B.; Vema, M.; Boddu, S. *Investigations on Spectroscopic Properties of Manganese Ions in Sodium Lead Alumino Borate Glasses*. preprint; Under Review, **2020**, https://doi.org/10.21203/rs.3.rs-49497/v1.
29. J Abhiram, J.; Thejas, R.; Ramakrishna, R.R.; Pattar, V.; Venugopal, A.R.; Rajashekara, K.M. Optical and structural properties of ZnO-SrO-B2O3 glasses. *AIP Conference Proceedings* **2020**, *2274*, https://doi.org/10.1063/5.0022415.
30. Cheng, Y.; Xiao, H.; Guo, W.; Guo, W. Structure and crystallization kinetics of PbO–B2O3 glasses. *Ceramics International* **2007**, *33*, 1341-1347, https://doi.org/10.1016/j.ceramint.2006.04.025.
31. Dahiya, J.; Malik, M.; Hooda, A.; Arzoo; Khasa, S. Influence of mixed transition ion on structural and optical properties of lithium bismuth borate glasses. *AIP Conference Proceedings* **2020**, *2265*, https://doi.org/10.1063/5.0017338.
32. El Batal, F.H.; El Kheshen, A.A.; Azooz, M.A.; Abo-Naf, S.M. Gamma Ray Interaction with Lithium Diborate Glasses Containing Transition Metals Ions. *Optical Materials* **2008**, *30*, 881–891, https://doi.org/10.1016/j.optmat.2007.03.010.
33. Viswanatha, R.; Reddy, M.V.S.; Reddy, C.N.; Chakradhar, R.P.S. Infrared and MAS NMR Studies of Potassium Borovanadate Glasses. *Journal of Molecular Structure* **2008**, *889*, 197–203, https://doi.org/10.1016/j.molstruc.2008.02.003.
34. Gandhi, Y.; Sudhakar, K. S. V.; Nagarjuna, M.; Veeraiah, N. Influence of WO3 on Some Physical Properties of MO–Sb2O3–B2O3 (M=Ca, Pb and Zn) Glass System. *Journal of Alloys and Compounds* **2009**, *485*, 876–886, https://doi.org/10.1016/j.jallcom.2009.06.115.
35. Sharma, G.; Singh, K.; Manupriya; Mohan, S.; Singh, H.; Bindra, S. Effects of Gamma Irradiation on Optical and Structural Properties of PbO–Bi2O3–B2O3 Glasses. *Radiation Physics and Chemistry* **2006**, *75*, 959–966, https://doi.org/10.1016/j.radphyschem.2006.02.008.
36. Thipperudra, A.; Manjunatha, S.; Pushpalatha, H.L.; Prashanth Kumar, M. DSC, FTIR Studies of Borophosphate Glasses Doped with SrO, Li_2O. *J. Phys.: Conf. Ser.* **2021**, *1921*, https://doi.org/10.1088/1742-6596/1921/1/012110.
37. Pothuganti, P.K; Bhogi, A.; Kalimi, M. R.; Reniguntla, P. Physical and Optical Properties of Borobismuthate Glasses Containing Vanadium Oxide. *Glass Phys Chem* **2020**, *46*, 146–154, https://doi.org/10.1134/S1087659620020078.
38. Srinivas, B.; Hameed, A.; Srinivas, G.; Narasimha Chary, M.; Shareefuddin, Md. Influence of V2O5 on Physical and Spectral (Optical, EPR & FTIR) Studies of SrO-TeO2-TiO2-B2O3 Glasses. *Optik* **2021**, *225*, https://doi.org/10.1016/j.ijleo.2020.165815.
39. Doweidar, H.; Saddeek, Y.B. FTIR and Ultrasonic Investigations on Modified Bismuth Borate Glasses. *Journal of Non-Crystalline Solids* **2009**, *355*, 348–354, https://doi.org/10.1016/j.jnoncrysol.2008.12.008.
40. Rada, S.; Pascuta, P.; Culea, M.; Maties, V.; Rada, M.; Barlea, M.; Culea, E. The Local Structure of Europium–Lead-Borate Glass Ceramics. *Journal of Molecular Structure* **2009**, *924–926*, 89–92, https://doi.org/10.1016/j.molstruc.2008.12.032.
41. El-Damrawi, G.; El-Egili, K. Characterization of Novel CeO2–B2O3 Glasses, Structure and Properties. *Physica B: Condensed Matter* **2001**, *299*, 180–186, https://doi.org/10.1016/S0921-4526(00)00593-7.
42. Bhogi, A.; Pothuganti, P.K.; Kistaiah, P. Structural properties of Li2O-BaO-B2O3-Fe2O3 glasses. *AIP Conference Proceedings* **2020**, *2220*, https://doi.org/10.1063/5.0001158.

43. Cozar, O.; Ardelean, I.; Bratu, I.; Simon, S.; Craciun, C.; David, L.; Cefan, C. IR and EPR Studies on Some Lithium-Borate Glasses with Vanadium Ions. *Journal of Molecular Structure* **2001**, *563–564*, 421–425, https://doi.org/10.1016/S0022-2860(01)00442-2.
44. Singh, S.; Kalia, G.; Singh, K. Effect of Intermediate Oxide (Y2O3) on Thermal, Structural and Optical Properties of Lithium Borosilicate Glasses. *Journal of Molecular Structure* **2015**, *1086*, 239–245, https://doi.org/10.1016/j.molstruc.2015.01.031.
45. Brow, R.K.; Tallant, D.R.; Turner, G.L. Polyhedral Arrangements in Lanthanum Aluminoborate Glasses. *Journal of the American Ceramic Society* **2005**, *80*, 1239–1244, https://doi.org/10.1111/j.1151-2916.1997.tb02970.x.
46. Maniu, D.; Iliescu, T.; Ardelean, I.; Cinta-Pinzaru, S.; Tarcea, N.; Kiefer, W. Raman Study on B2O3–CaO Glasses. *Journal of Molecular Structure* **2003**, *651–653*, 485–488, https://doi.org/10.1016/S0022-2860(03)00129-7.
47. Santos, C.N.; De Sousa Meneses, D.; Echegut, P.; Neuville, D.R.; Hernandes, A.C.; Ibanez, A. Structural, Dielectric, and Optical Properties of Yttrium Calcium Borate Glasses. *Appl. Phys. Lett.* **2009**, *94*, https://doi.org/10.1063/1.3115796.
48. Li, H.; Su, Y.; Li, L.; Strachan, D.M. Raman Spectroscopic Study of Gadolinium(III) in Sodium-Aluminoborosilicate Glasses. *Journal of Non-Crystalline Solids* **2001**, *292*, 167–176, https://doi.org/10.1016/S0022-3093(01)00878-X.
49. Hübert, T.; Mosel, G.; Witke, K. Structural Elements in Borovanadate Glasses. *Glass Physics and Chemistry* **2001**, *27*, 114–120, https://doi.org/10.1023/A:1011376225695.
50. Li, H.; Lin, H.; Chen, W.; Luo, L. IR and Raman Investigation on the Structure of (100-x)[0.33B2O3–0.67ZnO]–XV2O5 Glasses. *Journal of Non-Crystalline Solids* **2006**, *352*, 3069–3073, https://doi.org/10.1016/j.jnoncrysol.2006.03.073.
51. Padmaja, G.; Kistaiah, P. Infrared and Raman Spectroscopic Studies on Alkali Borate Glasses: Evidence of Mixed Alkali Effect. *J. Phys. Chem. A* **2009**, *113*, 2397–2404, https://doi.org/10.1021/jp809318e.
52. Chen, L.-T.; Lai, Y.-S. Thermal, Structural, and Metallization Properties of 0.95[50B2O3-30BaO-(20-x) ZnO-XBi2O3]+0.05V2O5 Glasses. *Journal of Non-Crystalline Solids* **2021**, *556*, https://doi.org/10.1016/j.jnoncrysol.2020.120552.